Please cite: Habermann, A.L., Zahn, R., Seitz, A., Hornung, M., "Multidimensional Parametric Study of a Propulsive Fuselage Concept Using OpenFOAM", AIAA AVIATION Conference, online, 2020, https://doi.org/10.2514/6.2020-2754

Multidimensional Parametric Study of a Propulsive Fuselage Concept Using OpenFOAM

A.L. Habermann*
Bauhaus Luftfahrt e.V., Taufkirchen, Bavaria, Germany

R. Zahn†
Technical University of Munich, Bavaria, Germany

A. Seitz‡, and M. Hornung§
Bauhaus Luftfahrt e.V., Taufkirchen, Bavaria, Germany

Aircraft concepts, which utilize boundary layer ingestion as a means to increase airframe and propulsion system integrated performance, such as propulsive fuselage concepts, have been the subject of many studies in the recent past. High fidelity numerical and experimental methods have been employed to optimize fuselage and propulsor geometries and performance characteristics. However, some of the fundamental principles that relate the physical shape of a fuselage-propulsor to the potential benefit of boundary layer ingestion are still not fully understood. The presented methodology serves as a tool to investigate the effect of geometrical propulsor parameters and fuselage-propulsor fan pressure ratio on the performance of a propulsive fuselage aircraft concept. For this purpose, a method for the systematic design space exploration of a fuselage-propulsor configuration is presented and applied in a 2D axisymmetric CFD study.

I. Nomenclature

∞, 0	=	freestream
A	=	area [m^2]
BLI	=	Boundary Layer Ingestion
BWB	=	Blended Wing Body
c	=	chord length [m]
CFD	=	Computational Fluid Dynamics
C_{hub}	=	fan hub constant [-]
C_f	=	skin friction coefficient [-]
C_p	=	pressure coefficient [-]
d	=	diameter [m]
DoE	=	Design of Experiment
$\eta_{p,fan}$	=	polytropic fan efficiency [-]
$f_{\eta,BLI}$	=	BLI efficiency factor [-]
F	=	Force [N]
FF	=	Fuselage Fan
FL	=	Flight Level [-]
FPR	=	Fan Pressure Ratio
fuse	=	fuselage
γ	=	isentropic coefficient [-]
h	=	height [m]
h	=	specific enthalpy [J/kg]

*Research Associate, Visionary Aircraft Concepts, AIAA Student Member.
†PhD student, Chair of Aerodynamics and Fluid Mechanics.
‡Deputy to Head of Visionary Aircraft Concepts, AIAA Member.
§Executive Director Research and Technology, AIAA Senior Member.

HiSA	=	High Speed Aerodynamic Solver
l	=	length [m]
LHS	=	Latin Hypercube Sampling
$\dot{m}$	=	mass flow [kg/s]
Ma	=	Mach number [-]
NPF	=	Net Propulsive Force [N]
NPP	=	Net Propulsive Power [W]
p_s	=	static pressure [Pa]
p_t	=	total pressure [Pa]
p_{t2}/p_{t0}	=	inlet total pressure recovery [-]
P	=	power [W]
P_s, $P_{s,a}$	=	actual shaft power [W]
$P_{s,s}$	=	isentropic shaft power [W]
ρ	=	density [kg/m$_2$]
PAX	=	passengers
PFC	=	Propulsive Fuselage Concept
Π_{fan}	=	fan pressure ratio [-]
r	=	radius [m]
RANS	=	Reynolds-Averaged Navier Stokes
RMSE	=	Root Mean Squared Error
S	=	surface area [m^2]
$_{surf}$	=	surface
SLR	=	SLenderness Ratio
TLAR	=	Top Level Aircraft Requirements
T_s	=	static temperature [K]
T_t	=	total temperature [K]
τ_w	=	wall shear stress [N]
U	=	velocity in flow direction [m/s]
$_x$	=	in flow direction
x_{fan}	=	axial fuselage fan position [-]
y^+	=	dimensionless wall distance [-]
$_z$	=	in axial direction

II. Introduction

Commercial aircraft concepts featuring a boundary layer ingesting (BLI) propulsive device, such as a fuselage fan (FF), have gained increasing attention in the recent years. The reduction of the momentum deficit induced by the fuselage boundary layer promises a high potential to decrease fuel burn. Prominent examples include the boundary layer ingesting aft-fuselage fan concept "Fuse Fan" by NASA [1], the Bauhaus Luftfahrt "Propulsive Fuselage" [2], the propulsive fuselage concepts (PFC) investigated in the European research projects "DisPURSAL" [3] and "CENTRELINE" [4], the NASA "STARC-ABL" [5], and the embedded BLI configuration "SAX-40" [6], and the "N3-X" (BWB) [7]. The expected fuel burn reduction potential of these concepts varies in the one digit range between 2-10% [3, 8–10] and even a predicted increase in fuel burn of 1.7% [11]. Top Level Aircraft Requirements (TLAR) as well as the aircraft and power train configuration and geometry of the concepts differ significantly. However, for all concepts the geometric shape of the fuselage and FF propulsion system plays an important role when optimizing a fuselage-propulsor concept for all design conditions, including cruise and off-design conditions. To maximize the benefit of such a concept design, it is necessary to optimize the shape from an aero-propulsive perspective.

For some of the introduced concepts, two- and three-dimensional geometry optimization schemes were applied in past studies. In 2001, Rodriguez conducted a two- and three-dimensional multidisciplinary design optimization of a BLI engine inlet of a blended wing body (BWB) with a Reynolds-Averaged Navier Stokes (RANS) solver. The study aimed at the demonstration of the potential advantages of BLI for BWB with a focus on engine inlet performance [12]. Gray et al. investigated the effect of fan pressure ratio (FPR) on the performance of the NASA STARC-ABL concept. They introduced a coupled-adjoint approach of a one-dimensional thermodynamic cycle coupled to a RANS CFD (Computational Fluid Dynamics) simulation. In their approach, the fuselage was modelled as two-dimensional and

axisymmetric, neglecting the effect of the wing on the propulsor performance. The aim of the study was to improve the performance of the BLI propulsor by optimizing the propulsor shape for a single design variable (FPR) [13, 14]. Kenway and Kiris also applied CFD on a simplified model of the NASA STARC-ABL concept. They performed a three-dimensional adjoint-based aerodynamic shape optimization of the fuselage diffuser and nacelle inlet to minimize inlet distortion at the BLI propulsor. Their results showed that the optimal nacelle and fuselage shape is very sensitive to flight conditions (Mach number, altitude, angle of attack) and wing downwash [15]. The shape optimization is, thus, a task specific to each BLI concept and its design conditions.

Rather than pursuing a localized geometric optimization of the aft-fuselage and propulsor shaping of a specific BLI configuration, the presented methodology aims at investigating the implications of the systematic variation of global design parameters on the integrated aero-propulsive aircraft performance of a full annular ducted PFC based on the CENTRELINE BLI configuration. For all configurations only a part of the boundary layer is ingested, never the full boundary layer or more. Three-dimensional effects such as effects of the wing downwash are not considered in the presented study.

For this purpose, the merit of a simple sensitivity study based on an initial geometry compared against a multidimensional design space exploration is investigated. A sensitivity analysis for six different geometrical and operational design variables is performed and complimented by a multidimensional parametric study of four key design parameters in order to find optimal design settings for the highest BLI benefit of an exemplary fuselage-propulsor geometry. One of the metrics used to compare the aero-propulsive benefit of different PFC designs is the bare BLI efficiency factor as defined by [16]. It relates the product of the net propulsive power to the ideal shaft power of the BLI propulsor. The net propulsive power is the product of net axial force (Net Propulsive Force - NPF) acting on the bare fuselage and nacelle arrangement (total surface and fan force) and the flight velocity. For a PFC, such as the CENTRELINE concept [4], a geometry shall be found with the highest NPF at the lowest shaft power expense.

The combination of the main study parameters (pressure ratio of the FF – FPR, axial fan position x_{fan}, fuselage slenderness ratio – SLR and FF duct height $h_{fan\ duct}$) in their specified ranges opens up a broad design space with possibly strong non-linear system behavior. However, at the conceptual stage only a limited number of high-fidelity simulation runs can typically be conducted from the perspective of computational resources and required calculation time. A solution to this problem is the application of an approximation-based optimization. As such, an analytic model typically referred to as "surrogate model" is derived to approximate the characteristics obtained from the high-fidelity model. The surrogate model is based on a limited number of high-fidelity simulation results. Its quality strongly depends on the appropriate distribution of sample points within the hyper-dimensional design space and therefore, requires the strategic placement of parameter combinations by the use of a space filling sampling technique. In the present study, a Latin Hypercube Sampling (LHS) strategy is applied [17, 18]. For the selected combinations, two-dimensional axisymmetric geometries based on a geometric parameterization of the geometry are generated and high-fidelity CFD simulations are executed for the design cruise condition. To solve the numerical problem, the open source CFD software OpenFOAM [19] is employed. A high speed aerodynamic solver (HiSA) is used, which was developed and validated by the Council for Scientific and Industrial Research in South Africa for the efficient and robust simulation of transonic and supersonic flows within OpenFOAM [20]. The impact of the propulsor on the fluid flow through the propulsor duct and the adjacent flow field is modelled by the application of first principle thermodynamic relations on a fan stage volume to capture the coupling effect of airframe aerodynamics and installed propulsion system performance [21].

Subsequently, the results of the simulations are processed serving as an input for the construction of a surrogate model, which is based on a Kriging approach. As part of the quality assurance process, the surrogate model is validated using both the results of the sensitivity study and the results of an independent set of data points obtained by the multidimensional CFD simulations.

Finally, a combination of parameters is identified that defines a global optimum of the given parameterized design within the design space, i.e. the two-dimensional propulsive fuselage geometry with the highest benefit compared to a two-dimensional reference fuselage.

III. Systematic Approach

The study follows a systematic approach as pictured in Figure 1.

During the design space definition, the two-dimensional axisymmetric baseline geometry of a generic BLI fuselage-propulsor configuration is derived. Its outline is based on the TLAR defined as part of the European research project CENTRELINE [4]. Serving the medium to long range wide-body aircraft segment, the CENTRELINE concept has a design range of 6500 nmi and a design payload of 340 PAX. The two-dimensional outline can be interpreted as the

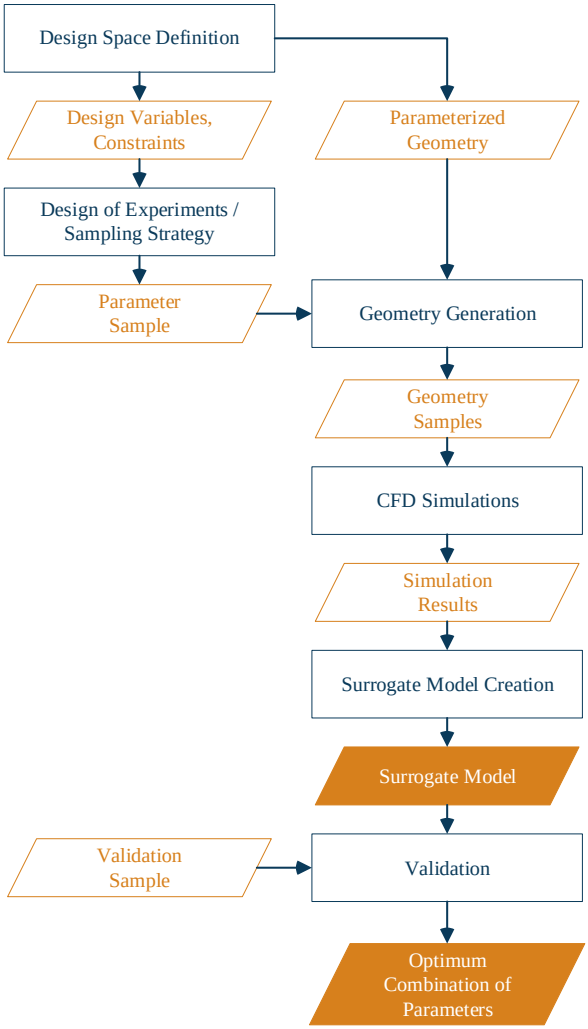

Fig. 1 Systematic approach.

top view cut through the aircraft fuselage presented in Figure 2. The geometry is parameterized following similarity heuristics (see section V). Design parameters deemed to have a crucial impact on the configuration's performance (see section IV.A) are identified and constrained to upper and lower limits as well as discrete intervals on account of engineering expertise.

Geometries are generated according to the parameter combination description and fed into a RANS CFD simulation. The simulation consists of three parts: pre-processing (meshing of the domain with Gmsh [22]), solving of the RANS equations using a simulation setup in OpenFOAM [19] and post-processing of the simulation results. The specifications of the simulation setup are described in section VI. The process is automated using the Python programming language, version 3.6 [23].

As the effects of all parameters on the aircraft performance are highly interdependent, each parameter is firstly varied independently around a reference value (see section VIII), and then varied in combination with the other parameters in a multidimensional parameter variation (see section IX).

The first step of the multidimensional parameter evaluation is the definition of a Design of Experiments (DoE) for which a Latin Hypercube Sampling strategy with maximized minimum distance between samples is chosen. Subsequent, simulation results of the sampled probe are fed into a Kriging surrogate model [24] (see section VII). A surrogate model, which covers the whole design space, is computed and validated against an additional validation sample and the results of the sensitivity study. Lastly, a set of design parameters is identified, which describes the configuration with a global aero-propulsive performance optimum.

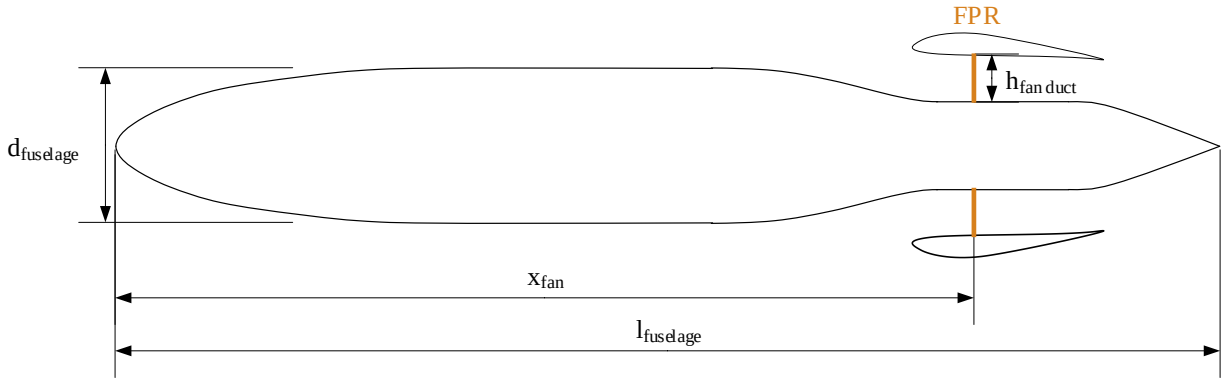

Fig. 2 Exemplary two-dimensional representation of the fuselage-propulsor concept and studied parameters.

Table 1 Design parameters considered in sensitivity study* and multi-dimensional design space exploration⁺.

Design Variable	Range	Baseline
Fan Pressure Ratio (FPR)*⁺ [-]	1.25 – 1.50	1.40
Axial Fuselage Fan Position (x_{fan})*⁺ [%]	85.0 - 95.0	90.0
Fuselage Length (l_{fuse})*⁺ [m]	60.0 - 70.0	67.0
Slenderness Ratio (SLR) [-]	9.15 - 13.96	12.47
Fuselage Fan Hub Coefficient (C_{hub})*⁺ [-]	0.20 - 0.40	0.25
Propulsor Fan Duct Height ($h_{fan\ duct}$) [m]	0.38 – 0.58	0.51
Mach Number (Ma)* [-]	0.78 – 0.84	0.82
Flight Level (FL)* [100 ft]	320 – 380	350

IV. Design Parameters and Performance Characteristics

As the aero-propulsive performance of the fuselage-propulsor configuration is highly dependent on its geometrical features, the present study focuses on the effect of geometric variation on both aerodynamic and propulsive performance characteristics described in the following section.

A. Design Parameters

The parametric study is based on a set of four design parameters with particularly strong impact on PFC geometric shape and aero-propulsive performance. The three defining geometric parameters are the duct height at the propulsor fan face ($h_{fan\ duct}$), the fuselage slenderness ratio (SLR = l_{fuse} / d_{fuse}), and the relative axial FF position x_{fan} as presented in Figure 2. The design FPR constitutes an additional important propulsion system related sizing parameter. A variation of the parameters cruise Mach number and cruise flight altitude provide an indication of possible operational strategies for a given geometry. The chosen parameterization method (see section V) makes it necessary to substitute the influential parameters SLR and $h_{fan\ duct}$ by the design parameters fuselage length l_{fuse} and a fan hub constant C_{hub}, which defines the ratio of maximum fuselage diameter and fan face hub diameter. Furthermore, the parameterization causes a strong coupling of the design parameters. Design parameter ranges and nominal values for the baseline geometry are given in Table 1. The baseline characteristics (geometry and FPR) are based on study results of the CENTRELINE configuration [4].

The slenderness ratio affects the development of the boundary layer before it reaches the FF. For a constant cabin floor area, the fuselage slenderness ratio determines the boundary layer thickness at the BLI propulsor intake: The smaller the SLR, the smaller the fuselage length compared to fuselage diameter. As the boundary layer thickness is a function of run length, the smaller the SLR, the smaller the boundary layer thickness at the propulsor inlet. The SLR is indirectly varied by a variation of l_{fuse} for a constant cabin floor area A_{cabin}. However, due to the chosen parameterization strategy, a variation of x_{fan} or C_{hub} also affect the SLR to a lesser extent.

The duct height at the FF face as well as the axial position of the fan determine the amount of boundary layer ingested by the FF.

As the fan face area itself is kept constant for all investigated geometries, the duct height is varied indirectly by a variation of the fan face duct radius through C_{hub}. The bigger the FF hub radius, the smaller the duct height. Thus, a smaller part of the boundary layer can be ingested.

The further upstream the propulsor is placed with respect to the total fuselage length, the smaller is the amount of total momentum losses resulting from the fuselage boundary layer, which can potentially be recovered by the fuselage aft fan. However, Smith pointed out that for an ideal wake-filling propulsor the propulsive efficiency is higher and the propulsor can be smaller for an ingestion of a wake with a higher shape factor, which is the case further upstream [25]. From an aircraft level perspective, the position of the fan is further constrained by a minimum angle of the propulsor aft cone, which prevents undesirable flow phenomena occurring in the propulsor jet. In addition, x_{fan} affects the shape of the fuselage. For the same total fuselage length, the maximum fuselage diameter can be smaller if the FF is placed further downstream at a constant cabin floor area. The axial fan face position is, thus, highly interdependent with the other design variables.

The FPR is a design variable, which again shows the strong coupling between airframe aerodynamics and aft propulsion system. At given freestream conditions, the FPR not only affects the performance of the propulsor, but also has a significant effect on the characteristics of the incident airflow. Gray et al. (2017) showed in a RANS CFD study of the NASA-STARC-ABL configuration that the performance of the BLI configuration is highly dependent on the FPR. They found that for their case at hand, the lower the FPR, the higher the net force acting on the propulsor-fuselage configuration [13].

B. Performance Characteristics

To compare the impact of the design variables on the configuration's aero-propulsive performance, the BLI benefit is evaluated with a metric that combines the effect of the propulsor on the airframe as well as the effect of the altered inflow on the propulsion system – the BLI efficiency factor as introduced in [16] and explained in [21]. It relates the product of the net propulsive power (NPP) to the isentropic shaft power expended in the fuselage-propulsor:

$$f_{\eta,BLI} = \frac{NPP}{P_{s,s}} \forall P_{s,s} > 0 \tag{1}$$

In the present study, the isentropic shaft power $P_{s,s}$ is replaced by the actual shaft power $P_s = P_{s,a}$, which is the isentropic shaft power corrected by the polytropic efficiency of the FF. Thus, the BLI efficiency factor used here will always perform worse compared against results of similar studies. As the polytropic fan efficiency is kept constant across all studied cases, the resulting trends, however, will be similar.

The NPP is the product of net axial force acting on the bare fuselage and propulsor arrangement ($\hat{=}$ NPF) and the freestream flight velocity: $NPP = NPF \cdot U_\infty$. The NPF is the sum of all axial forces acting on the configuration — pressure and viscous forces on all surfaces (fuselage, propulsor nacelle, propulsor duct, aft body) F_{surf} and the absolute value of the fan stage volume force F_{fan} . All surface forces are calculated by integration of the pressure and viscous forces on the surfaces. The contribution of the pressure and momentum flux of fan face and fan exit to the NPF is calculated from mass flow averaged values at propulsor stations 2 and 13 (see Figure 3). A negative NPF represents a force in drag direction.

$$NPF = |F_{fan}| - F_{surf} = \dot{m}(U_{13} - U_2) + A_{13}p_{s,13} - A_2 p_{s,2} - \sum_i \iint_{S_i} (p_s n_x + \tau_w)\, dS_i \tag{2}$$

The actual propulsor shaft power is determined in a similar manner from mass flow averaged propulsor station enthalpy:

$$P_s = \dot{m}(h_{13} - h_2) \tag{3}$$

For a given flight condition, the fuselage and FF nacelle force in drag direction should either be minimized for a given expended propulsor shaft power or a minimum shaft power should be expended for a given NPF. The performance characteristics serve as objective functions for the surrogate model designed in the multi-dimensional design space exploration.

In addition, the ratio of the mass-flow-averaged total pressure at the fuselage fan face and the freestream total pressure p_{t2}/p_{t0} is calculated [26]. The parameter describes the inlet total pressure recovery, which is caused by the

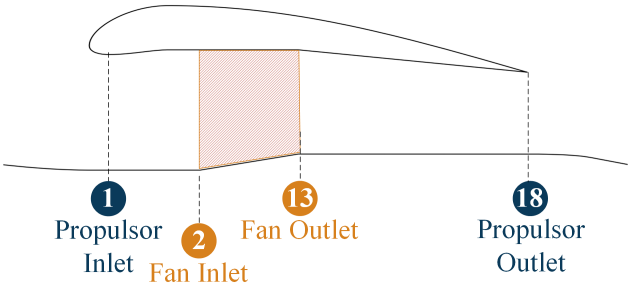

Fig. 3 Fuselage fan stations. In the present study, station 1 is defined as the location with the smallest area of the FF inlet duct. Adapted from [21].

fluid's propagation along the fuselage in front of the fan as well as the geometry of the propulsor inlet between FF highlight and station 2.

All performance parameters are calculated by an automated post-processing of the CFD results.

V. Geometry Parameterization

Exemplary mutations of the parameterized geometry are pictured in Figure 4. The 2D axisymmetric baseline configuration features a full annular ducted propulsor. The fuselage has an elliptical nose with $r_x = 3r_{fuse}$ and $r_z = r_{fuse}$ as well as a cylindrical center part. The aft fuselage geometry is determined by the propulsor design. In front of the propulsor, the cylindrical center section contracts from maximum fuselage radius to the propulsor hub radius in an S-shaped curve. For simplification reasons, the hub radius in front of the fan inlet and between fan outlet and nozzle exit is constant. Behind the propulsor, the fuselage contracts again, forming an aft cone. The baseline propulsor nacelle is designed in such a way, that no shocks occur on the outer contour for reference conditions (see section VIII.A).

To ensure comparability across the results, the following geometrical heuristics are implemented in the parameterized geometry description:

- 'Cabin floor area' similarity: The floor area of the vertical section through the symmetry line of the fuselage is kept constant at A_{cabin} = 260 m^2 as a first approximation of a constant number of passengers to be accomodated in the fuselage. In consequence, fuselage diameter and slenderness ratio are an output of the geometry generation (see section V).
- The angle of the fuselage contour leading to the propulsor inlet is held constant.
- The fan face duct height is indirectly varied with the design parameter C_{hub}, which defines the ratio of fan face hub height and maximum fuselage diameter.
- The position of the maximum nacelle thickness in percent nacelle chord length as well as the maximum nacelle thickness is constant.
- The ratio of the fan inlet tip radius to the nacelle chord length is constant.
- The angle of the outer nacelle contour trailing edge is constant.

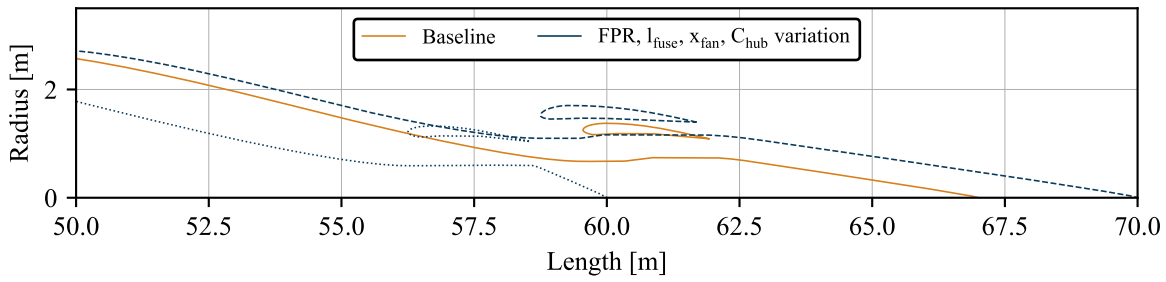

Fig. 4 Exemplary geometry mutations.

- Propulsor station areas: The areas of all propulsor stations are functions of the fan face area. Relationships are determined based on the local thermodynamic conditions and target axial flow Mach numbers at the individual stations. While design Mach numbers for the intake highlight and throat planes are prescribed, nozzle exit (station 18) Mach numbers result from the nozzle pressure ratios depending on flight speed, FPR and the total pressure losses in the streamtube.

VI. CFD Setup

Sensitivity study and surrogate model creation are based on results from RANS CFD simulations. The setup of the numerical simulations is described in the following.

A. Solver and Numerical Grid

In order to assess the flow around the fuselage-propulsor geometry, a high speed aerodynamics (HiSA) RANS solver is applied within OpenFOAM [20]. Turbulence is modelled using the k-ω-SST (Shear Stress Transport) model [27].

The free stream conditions are initialized using non-reflective far field boundary conditions. In order to account for a viscous flow around the propulsor nacelle and the fuselage, a no-slip condition is imposed on all surfaces. The flow conditions for the simulation are defined assuming FL350 and a free stream Mach number of 0.82 [4] (see Table 2).

Table 2 Freestream conditions.

Quantity	Value	Symbol
Mach number [-]	0.82	Ma_∞
Reynolds number [-]	$4.3 \cdot 10^8$	Re_∞
Gas constant [J/kg/K]	287.05	R
Specific heat ratio [-]	1.4	κ
Velocity [m/s]	243.16	U_∞
Density [kg/m^3]	0.3796	ρ_∞
Pressure [Pa]	23842	p_∞
Temperature [K]	218.81	T_∞
Turbulent kinetic energy [J/kg]	0.0887	k
Turbulent frequency [1/s]	54371	ω

The mesh is generated using the open source grid generator Gmsh [22]. The turbulent boundary layer is fully resolved with $y^+<1$ ($y^+_{ave}=0.4$ for the baseline geometry) as shown in Figure 5. Simulations are run for 12000 time steps to reach convergence.

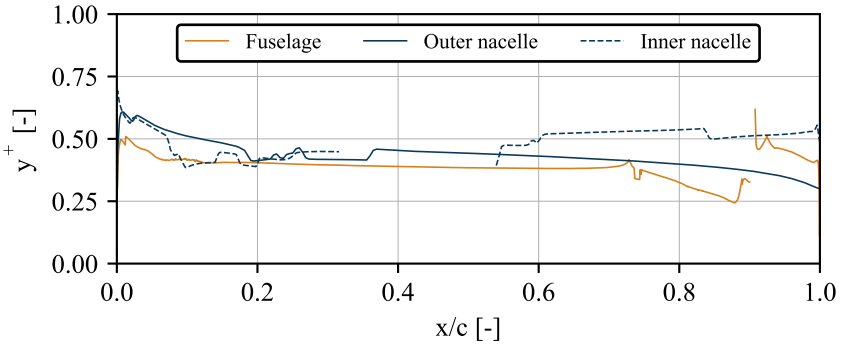

Fig. 5 y^+ distribution along fuselage and nacelle surface.

B. Fuselage Fan Model

The influence of the fan on the fluid flow is modeled by imposing customized boundary conditions based on fan inlet and outlet field values and given fan properties, which are described in [21]. The increase in total pressure and total temperature over the fan stage are defined by the fan pressure ratio Π_{fan} and the fan polytropic efficiency $\eta_{p,fan}$. A constant polytropic efficiency of 92.5% and constant FPR in radial direction are assumed in the first instance.

C. Validation

The HiSA solver has been validated for compressible, transonic flow conditions [28]. However, it was found that skin friction is not predicted by sufficient accuracy in a validation study of transonic airfoils [21]. Even though shocks were captured by CFD and the pressure distribution is sufficiently accurate, absolute drag was over predicted by 10-30% due to wall shear stress over-prediction independent of the employed turbulence model. It was found that the absolute skin friction surface force varies only by 2% compared against the absolute pressure surface force, which varies by up to 90% within the FPR range. Thus, it can be assumed that the propulsor has a significantly higher impact on the pressure distribution on fuselage and nacelle than on the skin friction distribution. Given the known inaccuracy, the simulation setup is deemed to be sufficient for the presented comparison of different geometries against a baseline geometry in a trend study.

VII. Sampling Strategy and Surrogate Model

In order to represent the design space as accurately as possible while keeping the computational effort at a low level, surrogate modeling is applied. In the present study, a surrogate model is computed based on a Kriging interpolation approach [24]. For this purpose, the Python Toolbox pyKriging [29] is used. The necessary sample data for the construction is defined by a number of evaluation points, which are equally distributed within the user-defined design space. Each evaluation point represents a different fuselage-propulsor configuration. In order to create a flexible sample plan independent of the number of design variables and the dimensionality of the design space, a LHS approach is applied.

By combining the different PFC configurations, which represent the system input, with the corresponding CFD solutions, the merged data set can be employed for surrogate model training purposes. For an efficient training computation, a gradient free genetic algorithm is applied. In the present study, 90% of the data set is used for the construction of the surrogate model, whereas the remaining percentage is applied for evaluation purposes. In addition, the computed Kriging model is validated based on the results of the sensitivity study. For this purpose, the root mean squared error (RMSE) of the Kriging model output and the reference CFD solution as obtained by both studies is calculated.

VIII. Sensitivity Study

A geometry suitable for the given TLAR serves as the baseline for the sensitivity study. Study parameters are varied independently around their baseline values. Results of the baseline geometry as well as some highlights of the sensitivity study are presented in the following. In addition, the best performing configuration based on the sensitivity study alone is identified.

A. Baseline Case

The baseline geometry (FPR=1.4, l_{fuse}=67m / SLR=12.47, x_{fan}=0.9, C_{hub}=0.25 / $h_{fan\ duct}$=0.51) experiences a NPF in drag direction of -8.3kN at an expended shaft power of 4.1MW. Compared to an axisymmetric non-BLI geometry with the same geometric dimensions, but without a FF (no nacelle and simplified, conical fuselage tail), the total force in drag direction is reduced by 10.2kN. However, the force is not fully recovered by the introduction of the FF. Compared to the non-BLI fuselage-propulsor configuration, the surface force on the fuselage decreases by 2.6kN and a nacelle surface force of 8.2kN is added. The nacelle force accounts for 34% of the total surface force. The inlet total pressure recovery is 88.3%.

Regions of high subsonic Mach numbers occur on the outer FF nacelle geometry and the inside of the FF lip. The flow separates at the aft tail of the fuselage as presented in Figure 6.

In front of the FF, pressure increases due to the suction effect of the FF (see Figure 7, top).

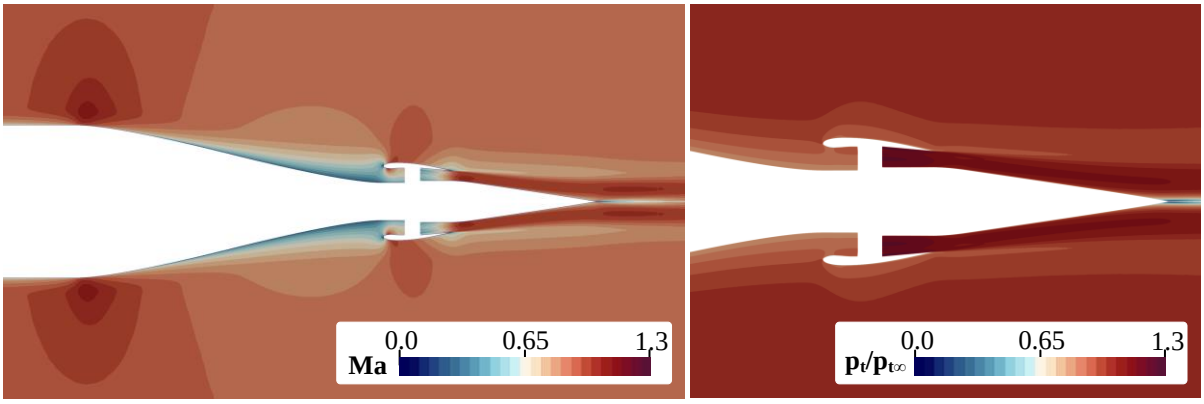

Fig. 6 Mach number and total pressure distribution of baseline geometry.

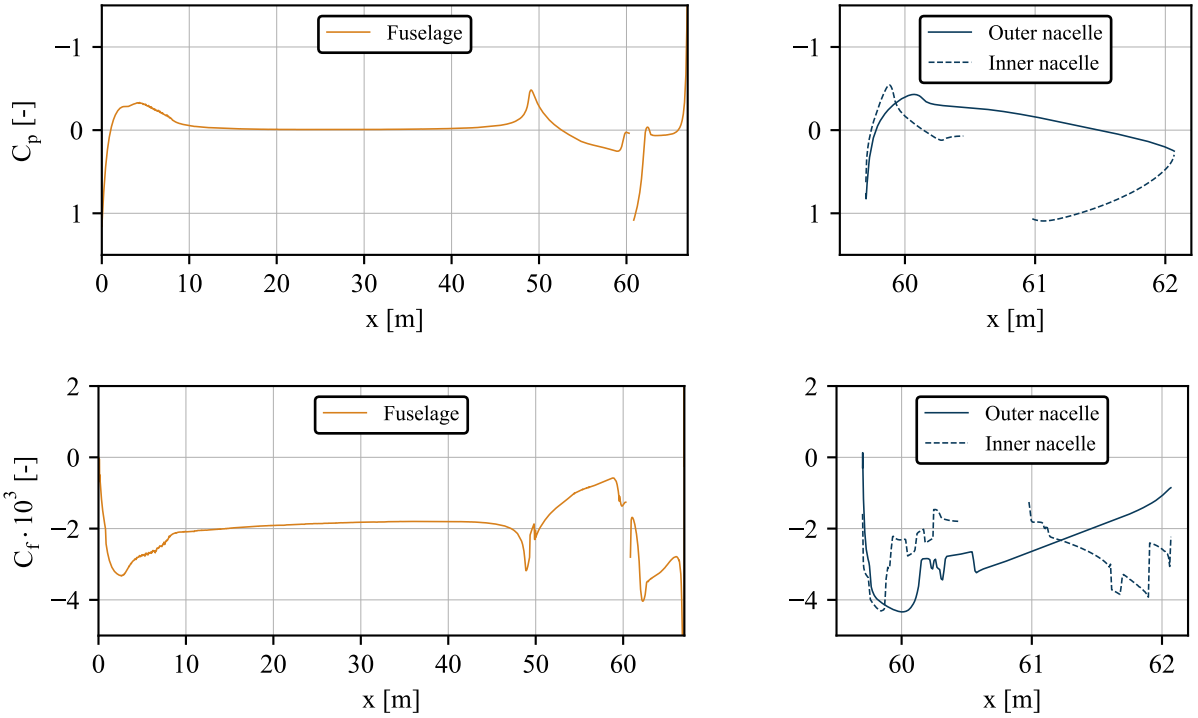

Fig. 7 Pressure and skin friction coefficient distribution along nacelle and fuselage for baseline geometry.

B. Study Results

The baseline geometry features parameters, which are manually optimized for the given operating conditions and constraints. Thus, a bias in the results is expected. As obvious from the results of the sensitivity study presented in Figures 10 and 11, the baseline geometry, marked in green in all figures, performs different from the parametrically derived variants. Therefore, all presented curve fits exclude the results of the reference geometry. Curves are fitted using simple linear regression with linear, potential, 2nd or 3rd order polynomial terms .

The NPF remains negative (force in drag direction) for all studied cases, because the FF force is always smaller than the total surface force. Even drastic changes in the geometry or FPR show only a small effect on the inlet pressure recovery of +0.26/-0.52%.

Varying the FPR has the biggest impact on the performance of the fuselage-propulsor body, especially on the shaft power required by the FF as depicted in Figure 10 – a 10% reduction of the baseline FPR leads to a 36% reduction of

the expended shaft power. The results indicate an opposing trend to the results presented by Gray et al. 2017 [13], who showed that the net axial force in thrust directions decreases with increasing FPR. The deviation of the results is caused by the differing study objectives. Gray et al. assumed a constant FF shaft power for all studies compared against the fixed FF inlet area assumed in the present study. In consequence, in Gray et al.'s study the nacelle is moved further inward for increasing FPR and, thus, more deeply embedded in the boundary layer – the nacelle surface force decreases. In contrast, the main cause for the increase in surface force with increasing FPR in the present study is the almost linear rise in nacelle surface force, which is eventually caused by the geometry parameterization strategy. The fan face area is kept constant across the study and only the fan exit and nozzle exit area are reduced for larger FPR. Due to the suction effect of the fan, the flow velocity inside the FF duct is higher for bigger FPR and, thus, the nacelle surface force increases.

Increasing the fuselage length/SLR results in a reduction of the total surface force. This is caused by a decrease in fuselage and nacelle surface area – at a constant cabin floor area, the fuselage radius is reduced at a higher rate than the fuselage length is increased. At the same time, the fan volume force increases for some of the cases.

C_{hub}/fan face duct height variation at constant fan face area leads to the highest variation of the total surface force, which is caused by a significant increase of the nacelle surface force. The bigger C_{hub}, the smaller the distance of the nacelle to the fuselage surface. At a constant fan face area, the nacelle is located further outward with respect to the centerline of the fuselage. The contraction of the fuselage geometry in front of the propulsor is weaker and the boundary layer thickness increases less. Thus, the nacelle is placed in a region of faster mass flow averaged fluid flow and experiences a higher surface force.

The further aft the FF is located with respect to the total fuselage length, the smaller the fuselage surface force. The force decreases proportionally with the fuselage surface area. At a constant cabin area, the fuselage radius can be smaller when the fan is located further downstream. Accordingly, the surface area is reduced and, correspondingly, the fuselage surface force. Fan volume force and expended shaft power show a maximum near a fan axial position of 89% fuselage length. This trend cannot be reproduced in the multidimensional parameter variation (see section IX.A).

Overall, the correlation of the geometrical parameters and the FPR with the fan volume force is less pronounced than the corresponding total surface force or inlet total pressure recovery.

A variation of the freestream characteristics effect surface and fan volume force in a similar manner. An increase in Ma number results in an increased surface and fan volume force. Results indicate, that the inlet pressure recovery decreases with an increase of Mach number or flight altitude. The trends are caused by opposing effects – p_{t2} and p_{t0} both increase with increasing Ma number, while they both decrease with increasing flight altitude to a different extent. As the mass flow through the propulsor decreases with increasing altitude, the expended shaft power decreases proportionally.

C. Best Performing Configuration

The objective of the aerodynamic design optimzation is to find a fuselage-propulsor geometry, which reduces the force in drag direction the most at the least expense of FF shaft power. An evaluation of the sensitivity study results alone shows, that the configuration with the smallest force in drag direction is the one with the longest fuselage length due to a combination of small surface force and high fan force (FPR=1.4, l_{fuse}=70m, x_{fan}=0.9, C_{hub}=0.25). The geometry also features the second best BLI efficiency factor ($f_{\eta,BLI}$=-0.239 at P_s=4.00MW) and the highest inlet total pressure recovery value (p_{t2}/p_{t0}=88.73%). The best BLI efficiency factor results from the geometry with the highest FPR. However, the fuselage-propulsor requires 1.82MW more shaft power ($f_{\eta,BLI}$=-0.226 at P_s=5.82MW). At the smallest FPR, which is considered in the present study, the least FF shaft power is expended. At the same time, the FF recovers only little force in drag direction and, thus, shows a high BLI efficiency factor. In conclusion, as a result of the sensitivity study, the configuration with the parameters FPR=1.4, l_{fuse}=70m, x_{fan}=0.9, C_{hub}=0.25 is deemed to be the best from an aircraft level perspective.

IX. Multidimensional Design Space Exploration

Subsequent to the sensitivity study, a multidimensional parameter study based on a Kriging surrogate model is performed. The analyzed design space is represented by different fuselage-propulsor configurations, resulting from the aforementioned sampling strategy (see section VII). In order to receive a sufficient representation of the overall design space, a data set of 100 configurations is defined, of which 98% converged in the CFD simulations. In Figure 8, the distribution of the sample data points in the four-dimensional design space is visualized (top four rows). In order to define the input for the Kriging model, the resulting configurations are investigated by means of RANS

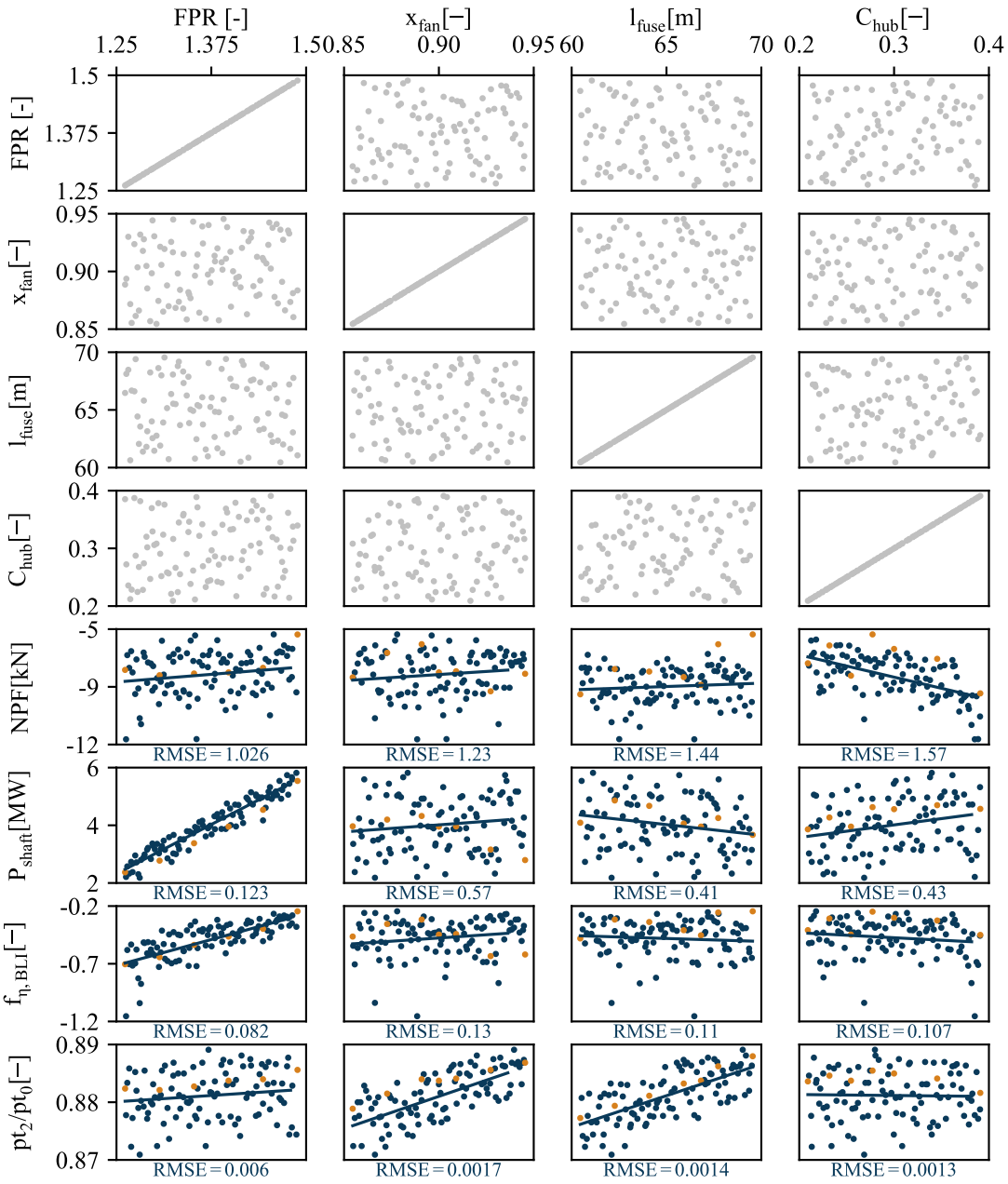

Fig. 8 Summary of sample distributions (gray) and results obtained by the sensitivity study (orange) and the multiparameter study (blue).

Table 3 RMSE of Kriging models and the CFD reference solution of multidimensional training data.

Kriging model	**RMSE** [-]
K_{P_s}	0.145
K_{NPF}	0.362
$K_{p_{t2}/p_{t0}}$	0.002

CFD simulations. Since the application of the Kriging model aims at defining the configuration with the highest aero-propulsive performance and in order to account for non-linearity in the defined design space, FF shaft power and NPF serve as separate objective functions of the model. In addition, a Kriging model ($K_{p_{t2}/p_{t0}}$) for the prediction of inlet total pressure recovery is evaluated. Each model is individually trained and validated. After a successful validation procedure, the Kriging models of FF shaft power (K_{P_s}) and NPF (K_{NPF}) are combined for further application. The evaluation of each model's quality is accomplished based on the results of the sensitivity study and a fraction of the training data of the multidimensional study, as described in section VII. The resulting RMSE of the Kriging models and the CFD solution of the sensitivity study are depicted in Figure 8. In Table 3, the RMSE of each Kriging model and the CFD solution of the multidimensional validation data set are summarized. Based on the computed prediction errors, the Kriging models are deemed to be sufficiently accurate for the following design space exploration.

A. Study Results

Prior to performing the design optimization, the results of the investigated fuselage-propulsor configurations, as shown in Figure 8, are discussed in the following. All configurations experience a net axial force in drag direction.

As already indicated by the sensitivity study, a variation in FPR influences the performance of the fuselage-propulsor configuration most, in particular the shaft power required to operate the FF. However, the impact on NPF is less distinctive. In contrast, the influence of the remaining design parameters on power requirement and NPF is less pronounced but rather indicates a higher interconnection of the design parameters with each other. Only a variation of the fan hub constant shows a measurable impact on the NPF, which substantiates the indications of the sensitivity study.

Concerning the recovery of inlet total pressure, only a minor impact of FPR is apparent, whereas a variation in axial fan position and fuselage length indicate distinct effects. As depicted in Figure 8, increasing the length of the fuselage and moving the position of the fan further downstream, result in an increase in inlet pressure recovery. These trends confirm the trends indicative of the sensitivity study.

In order to gain a deeper understanding of the interconnected influence of the selected design parameters on the performance of the PFC, the configurations with the lowest and highest FF shaft power, NPF, BLI efficiency factor

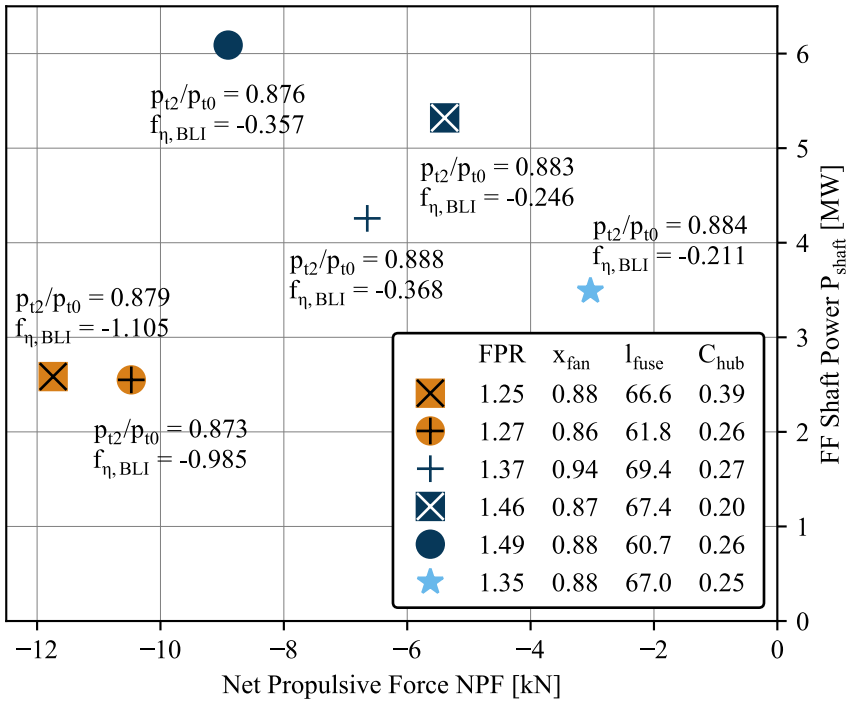

Fig. 9 Comparison of configurations with highest (blue) and lowest (orange) Net Propulsive Force (×), FF Shaft Power (○), BLI Efficiency (□) and FF Pressure Ratio (+). Optimized configuration (⋆).

and inlet pressure recovery are summarized in Figure 9. The configuration with the highest BLI efficiency factor ($f_{\eta,BLI}$=-0.246 at P_s=5.32MW and NPF=-5.39kN; force in drag direction) is characterized by a comparatively high FPR (FPR=1.46), a medium fuselage length (l_{fuse}=67.4m), a forward positioned fan (x_{fan}=0.87) as well as the smallest possible fan hub constant (C_{hub}=0.25). Further, the configuration provides a high inlet pressure recovery of p_{t2}/p_{t0}=88.3%. Again, the configuration with the best combined aero-propulsive performance requires a high FF shaft power compared to other configurations. In contrast, the geometry indicating the lowest BLI efficiency factor ($f_{\eta,BLI}$=-1.105 at P_s=2.58MW and NPF=-11.94 kN) is specified by a considerably lower FPR of 1.25 and a higher fan face hub constant of C_{hub} = 0.39. However, fuselage length and fan position are similar compared to the configuration featuring the best $f_{\eta,BLI}$. Inlet total pressure recovery decreases by 0.4% to p_{t2}/p_{t0}=87.9%.

Concerning the recovery of inlet pressure, the most efficient configuration is characterized by a medium FPR (FPR=1.37), a medium fan hub constant (C_{hub}=0.27), a long fuselage (l_{fuse}=69.4m) as well as a downstream positioned fan (x_{fan}=0.94). In contrast, a configuration defined by a short fuselage (l_{fuse}=61.8m) and an upstream positioned fan (x_{fan}=0.86) indicates a loss in inlet pressure recovery of almost 1.5% compared to the configuration with the highest inlet pressure recovery (p_{t2}/p_{t0}=87.3%). In addition, the geometry is characterized by a considerably lower FPR (FPR=1.27) and a similar fan hub constant (C_{hub}=0.26), resulting in a lower shaft power and only a moderately higher NPF.

Similar to the results of the sensitivity study, the configurations requiring the least FF shaft power show a bad aero-propulsive performance.

Based on the studied configurations, a correlation between FPR and shaft power is clearly visible as shown in Figure 9. The highest influence on NPF is indicated by changing the fan hub constant, whereas variations in fuselage length and axial fan position affect the recovery of inlet pressure most.

The results of the best parameter combinations compare well for small shaft power values with the BLI efficiency factor versus FF shaft power heuristics derived in Seitz et al. [8]

B. Design Optimization

In order to identify the configuration characterized by the best BLI efficiency, the combined trained and validated Kriging model is employed. As a result of the Kriging optimization, the configuration with the best BLI efficiency factor ($f_{\eta,BLI}$=-0.211 at P_s=3.49MW and NPF=-3.03 kN) is defined by a FPR of 1.35, a fuselage length of l_{fuse}=67m, an axial fan position of x_{fan}=0.88 and a fan hub constant of C_{hub}=0.25. The inlet pressure recovery is computed as p_{t2}/p_{t0}=88.4%. Compared against the pure evaluation of the cases, which were used for the training of the Kriging model, a design could be found, which shows a better aero-propulsive performance at a smaller expended FF shaft power (see section IX.A).

X. Discussion

A comparison of sensitivity study and multidimensional design space exploration results evaluates the additional value of a coupled design parameter variation. Design implications for the presented fuselage-propulsor configuration are identified and limitations of the applicability of the results to other PFC configurations are reported.

A. Comparison of Sensitivity Study and Multidimensional Study Results

All presented results demonstrate the strong dependency of the coupled aerodynamic and propulsive performance of a PFC on the pre-defined FF operating conditions (FPR) and the geometric features of the fuselage-propulsor configuration. Choosing a best and balanced combination of design parameters is, therefore, crucial to ensure its optimal performance.

Comparing the results of sensitivity study and multidimensional design space exploration shows that a sensitivity study can be a good approach to get a first understanding of the magnitude of effects design parameters have on the aero-propulsive performance of an initially defined configuration. Most trends indicated by the sensitivity study results are matched by the Kriging model constructed from the multidimensional design space exploration. Yet, the high degree of coupling of the design parameters makes a multidimensional variation of the parameters inevitable in order to find the best combination of parameters for given TLAR and operating conditions.

The fairly scattered results of the multidisciplinary study indicate that for almost every parameter specification in the given value range (x_{fan}, l_{fuse},C_{hub}) a geometry exists, which shows a good aero-propulsive performance with a $f_{\eta,BLI}$ close to -0.2. The scattering also shows that the performance of the geometry is highly dependent on a well-chosen set of parameters depending on the TLAR constraints imposed on the design.

The evaluation of both, variation of design parameters in a sensitivity study and in a more complex multidimensional

Table 4 Baseline and best performing configuration resulting from sensitivity and multidisciplinary study.

	FPR [-]	x_{fan} [-]	l_{fuse} [m]	C_{hub} [-]	NPF [kN]	P_{shaft} [MW]	$f_{\eta,BLI}$ [-]	p_{t2}/p_{t0} [-]
Baseline	1.40	0.90	67.0	0.25	-8.31	4.14	-0.49	0.88
Sensitivity	1.40	0.90	70.0	0.25	-3.93	4.00	-0.24	0.89
Multidim.	1.35	0.88	67.0	0.25	-3.03	3.49	-0.21	0.88

study, result in configurations, which perform better than the baseline fuselage-propulsor geometry. In both studies, configurations can be identified, which show a smaller expended shaft power at a better aero-propulsive performance (see Table 4). Interestingly, the best configurations differ only slightly from the baseline configuration in terms of design parameters. This might be caused by the bias, which was introduced when defining the baseline geometry. The training and evaluation of the Kriging model was successful in finding a design parameter combination, which leads to a better performing configuration than the one, which could be found by evaluating the sensitivity study results alone. The fuselage-propulsor configuration, which is performing best features a FPR of 1.35.

In summary, relying on the results of a sensitivity study alone might not lead to the identification of the best performing fuselage-propulsor configuration. As the impact of the design parameters on the performance is highly coupled, it will be necessary to not only create a surrogate model from the variation of a few design parameters, but to perform a design optimization based on a higher number of geometric parameters including parameters, which describe the shape of the FF cowling.

B. Design Implications

For most of the design parameters, no conclusive design implications can be identified, which are valid for any PFC configuration. This is mainly caused by the selected parameterization strategy. However, some design rules can be derived, which hold true for the presented fuselage-propulsor configuration and have to be re-evaluated if applied to other designs.

Compared to all other metrics, the inlet total pressure recovery shows the most distinct (almost linear) dependency on the design parameters. The metric gives an indication of the impact of the fuselage geometry on the boundary layer incident to the FF. A higher p_{t2}/p_{t0} describes a smaller two-dimensional momentum deficit incident to the FF. The trends for both, sensitivity study and multidimensional design space exploration, point in a similar direction. Independent of fuselage length, axial fan position and corresponding inlet total pressure recovery, parameter combinations can be identified, which show a good aero-propulsive performance (see Figure 8).

When it comes to the fuselage length, the obtained results suggest that slender (longer) fuselages are favorable compared to those with a bigger maximum diameter as they show a smaller net force in drag direction at a smaller shaft power expense.

Placing the FF further downstream of the fuselage can result in the occurrence of unwanted regions of high Mach number at the steep fuselage aft cone as a direct result of the geometric parameterization strategy. Nevertheless, due to the assumption of constant cabin floor area, the total fuselage length can be reduced at the same time and, thus, the aero-propulsive performance is increased.

For a long haul aircraft, such as the CENTRELINE concept, the cruise conditions serve as the defining conditions for the optimization of the fuselage-propulsor configuration as most fuel is burned during this flight segment. Therefore, design cruise conditions, including the FPR of the aft propulsor and the operating conditions have to be chosen carefully and the geometry has to be optimized for these conditions.

Choosing a design FPR for the FF has crucial implications on the overall performance of a PFC aircraft. A compromise has to be made between a high aero-propulsive performance of the fuselage-propulsor configuration (optimum BLI efficiency factor) and the performance of the aircraft propulsion system. Numerical results indicate that increasing the FPR effects a steeper increase in expended FF shaft power compared to the reduction in NPF in drag direction and that a smaller design FPR could be preferable. However, design effects on aircraft level have to be considered, such as fan stability, FF inflow distortion tolerance, FF efficiency or FF installation and cascade mass effects.

Knowledge about the behavior of the propulsor-fuselage configuration at different freestream conditions, such as a different cruise speed or flight altitude can help to identify TLAR for a promising propulsive fuselage application. For the studied geometry, a lower cruise altitude and cruise Mach number seem favorable.

In general, for every new application case, a parameter optimization will be necessary in order to identify the design parameter combination corresponding to the best performing fuselage-propulsor configuration. The results of the

presented study can, however, serve as a help for the definition of the baseline geometry and the limitation of the design parameters.

C. Limitations

The applicability of the presented study results to fuselage-propulsor configurations of other PFC aircraft is limited by several factors. Most of them are related to the selected parameterization method and the strong interdependence of the chosen design parameters.

For all cases the force in drag direction cannot be compensated by the FF. Among other reasons, this is caused by a disadvantageous initial definition of the fan face area, which remained unchanged for all studied geometries. In future studies, the parameterization strategy has to be adjusted in a way that the FF area and other parameters, which define the aft propulsor geometry, is iteratively adapted to the present flow conditions. This may be achieved through a coupling of the RANS CFD simulation with a thermodynamic cycle, such as presented by Gray et al. [13].

In addition, the approach has to be expanded to include more design parameters. These have to include parameters, which describe the shape of the FF nacelle, the contour of the fuselage in front of the FF and inside the propulsor duct. A full parameterization of the geometry will also result in a lower interdependency of the design parameters.

Ultimately, a three-dimensional optimization of the geometry will be inevitable. This will include a three-dimensional fuselage, a three-dimensional FF nacelle, as well as all other aircraft components, which have an effect on the FF inlet distortion.

Even though cruise is the crucial condition for long haul aircraft from an aerodynamic performance perspective, it also has to be shown that the FF is operable with a sufficient efficiency and operational stability for all other operating conditions, including sideslip angles and take-off with ground effect.

XI. Conclusion

The presented study focused on the development of a systematic approach to identify physical relations between design parameters of a propulsive fuselage concept fuselage-propulsor configuration and its aero-propulsive performance. Prior to the creation of a surrogate model based on the results of a multidimensional design space exploration, the effect of an independent variation of design parameters around a baseline configuration was investigated. Results of the sensitivity study indicated that compared to the geometrical parameters (fuselage length, axial fan position and aft propulsor duct height), the fan pressure ratio of the fuselage fan has the biggest impact on the performance of the fuselage-propulsor body, especially on the shaft power required by the fuselage fan from the underwing podded engines. The axial net propulsive force on the body, however, can be manipulated to a high degree by a well-designed geometry. The results of the multiparameter study suggested a strong interconnection of the design parameters, which is partially caused by the selected geometry parameterization strategy. The simultaneous variation of the design parameters reproduced similar trends compared to the sensitivity study, but a better performing geometry composed of a different combination of design parameters could be identified. It was shown that a numerical multidimensional design space exploration of the fuselage-propulsor geometry, similar to the presented approach, can be useful to identify an optimally designed boundary layer ingesting fuselage fan.

Acknowledgments

This work is conducted within the CENTRELINE project, which has received funding from the European Union's Horizon 2020 research and innovation programme under Grant Agreement No. 723242. We would like to thank Anubhav Gokhale and Julian Bijewitz for their contribution to the study.

References

[1] Bolonkin, A., "A high efficiency fuselage propeller ('Fusefan') for Subsonic Aircraft," *SAE Technical Paper*, , No. 1991-01-5569, 1999.

[2] Steiner, H.-J., Seitz, A., Wieczorek, K., Plötner, K., Isikveren, A. T., and Hornung, M., "Multi-disciplinary Design and Feasibility Study of Distributed Propulsion Systems," *28th International Congress of the Aeronautical Sciences*, 2012.

[3] Isikveren, A. T., Seitz, A., Bijewitz, J., Mirzoyan, A., Isyanoc, A., Grenon, R., Atinault, O., Godard, J.-L., and Stückl, S.,

"Distributed propulsion and ultra-high by-pass rotor study at aircraft level," *The Aeronautical Journal*, Vol. 119, No. 1221, 2015, pp. 1327–1376.

[4] Seitz, A., Peter, F., Bijewitz, J., Habermann, A. L., Goraj, Z., Kowalski, M., Castillo Pardo, A., Hall, C., Meller, F., Merkler, R., Petit, O., Samuelsson, S., Della Corte, B., van Sluis, M., Wortmann, G., and Dietz, M., "Concept Validation Study for Fuselage Wake-Filling Propulsion Integration," *31st Congress of the International Council of the Aeronautical Sciences*, 2018.

[5] Welstead, J. R., and Felder, J. L., "Conceptual Design of a Single-Aisle Turboelectric Commercial Transport with Fuselage Boundary Layer Ingestion," *AIAA*, 2016.

[6] de La Rosa, E., Hall, C., and Crichto, D., "Special session – towards a silent aircraft challenges in the silent aircraft engine design," *45th AIAA Aerospace Sciences Meeting and Exhibit,*, 2002.

[7] Armstrong, M. J., Ross, C. A., Blackwelder, M. J., and Rajashekara, K., "Trade studies for NASA N3-X turboelectric distributed propulsion system electrical power system architecture," *SAE International Journal of Aerospace*, Vol. 5, No. 2012-01-2163, 2012, pp. 325–336.

[8] Seitz, A., Habermann, A. L., and van Sluis, M., "Optimality considerations for propulsive fuselage power savings," *Proc. IMech, Part G: J Aerospace Engineering*, 2020. doi:10.1177/0954410020916319.

[9] Hardin, L., Tillman, G., Sharma, O., Berton, J., and Arend, D., "Aircraft System Study of Boundary Layer Ingesting Propulsion," *48th AIAA/ASME/SAE/ASEE Joint Propulsion Conference & Exhibit*, American Institute of Aeronautics and Astronautics, Reston, Virigina, 2012. doi:10.2514/6.2012-3993.

[10] Welstead, J., Felder, J., Guynn, M., Haller, B., Tong, M., Jones, S., Gray, J. S., Ordaz, I., Quinlan, J., Mason, B., Schnulo, S., and Sil, A., "Overview of the NASA STARC-ABL (Rev. B) Advanced Concept," , 30.5.2018.

[11] Giannakakis, P., Maldonado, Y.-B., Tantot, N., Frantz, C., and Belleville, M., "Fuel burn evaluation of a turbo-electric propulsive fuselage aircraft," *AIAA Propulsion and Energy 2019 Forum*, American Institute of Aeronautics and Astronautics, Reston, Virginia, 2019, p. 1992. doi:10.2514/6.2019-4181.

[12] Rodriguez, D. L., "A multidisciplinary optimization method for designing boundary layer ingesting inlets," Dissertation, Stanford University, 2001.

[13] Gray, J. S., Mader, C. A., Kenway, G. K. W., and Martins, J. R. R. A., "Modeling Boundary Layer Ingestion Using a Coupled Aeropropulsive Analysis," *Journal of Aircraft*, Vol. 55, No. 3, 2017b, pp. 1191–1199. doi:10.2514/1.C034601.

[14] Gray, J. S., and Martins, J. R. R. A., "Coupled aeropropulsive design optimisation of a boundary-layer ingestion propulsor," *The Aeronautical Journal*, Vol. 30, 2018, pp. 1–17. doi:10.1017/aer.2018.120.

[15] Kenway, G. K., and Kiris, C. C., "Aerodynamic Shape Optimization of the STARC-ABL Concept for Minimal Inlet Distortion," 2018. doi:10.2514/6.2018-1912.

[16] Habermann, A. L., Bijewitz, J., Seitz, A., and Hornung, M., "Performance Bookkeeping for Aircraft Configurations with Fuselage Wake-Filling Propulsion Integration," *CEAS Aeronautical Journal*, 2019.

[17] McKay, M. D., Beckman, R. J., and Conover, W. J., "A comparison of three methods for selecting values of input variables in the analysis of output from a computer code," *Technometrics*, Vol. 42, No. 1, 2000, pp. 55–61.

[18] Press, W. H., Teukolsky, S. A., Vetterling, W. T., and Flannery, B. P., *Numerical recipes 3rd edition: The art of scientific computing*, Cambridge university press, 2007.

[19] Weller, H. G., Tabor, G., Jasak, H., and Fureby, C., "A tensorial approach to computational continuum mechanics using object-oriented techniques," *Computers in Physics*, Vol. 12, No. 6, 1998, p. 620. doi:10.1063/1.168744.

[20] J.A. Heyns, O.F. Oxtoby, A. Steenkamp, "Modelling high-speed flow using a matrix-free coupled solver," , 23-26 June 2014.

[21] Habermann, A. L., Gokhale, A., and Hornung, M., "Numerical Investigation of the Effects of Fuselage Upsweep in a Propulsive Fuselage Concept," *1st Aerospace Europe Conference*, 2020.

[22] Geuzaine, C., and Remacle, J.-F., "Gmsh: a three-dimensional finite element mesh generator withbuilt-in pre- and post-processing facilities," *International Journal for Numerical Methods in Engineering*, Vol. 79, No. 11, 2009, pp. 1309–1331.

[23] "Python, Version 3.6," , 04/28/2020. URL `https://www.python.org/`.

[24] Forrester, A., Sobester, A., and Keane, A., *Engineering Design via Surrogate Modelling: A Practical Guide*, John Wiley & Sons Ltd., 2008.

[25] Smith, L. H., "Wake Ingestion Propulsion Benefit," 1993.

[26] Seitz, A., and Gologan, C., "Parametric Design Studies for Propulsive Fuselage Aircraft Concepts," *4th CEAS Air Space Conference*, 2013.

[27] F.R. Menter, M. Kuntz, R. Langtry, "Ten years of industrial experience with the SST turbulence model," *Turbulence, Heat and Mass Transfer*, Vol. 1, No. 4, 2003, pp. 624–632.

[28] "Hisa: CFD Verification and Validation Archive," , 04/28/2020. URL `http://hisa.gitlab.io/archive.html`.

[29] "pyKriging - a User Friendly Python Kriging ToolBox," , 04/30/2020. URL `http://pykriging.com/`.

Appendix

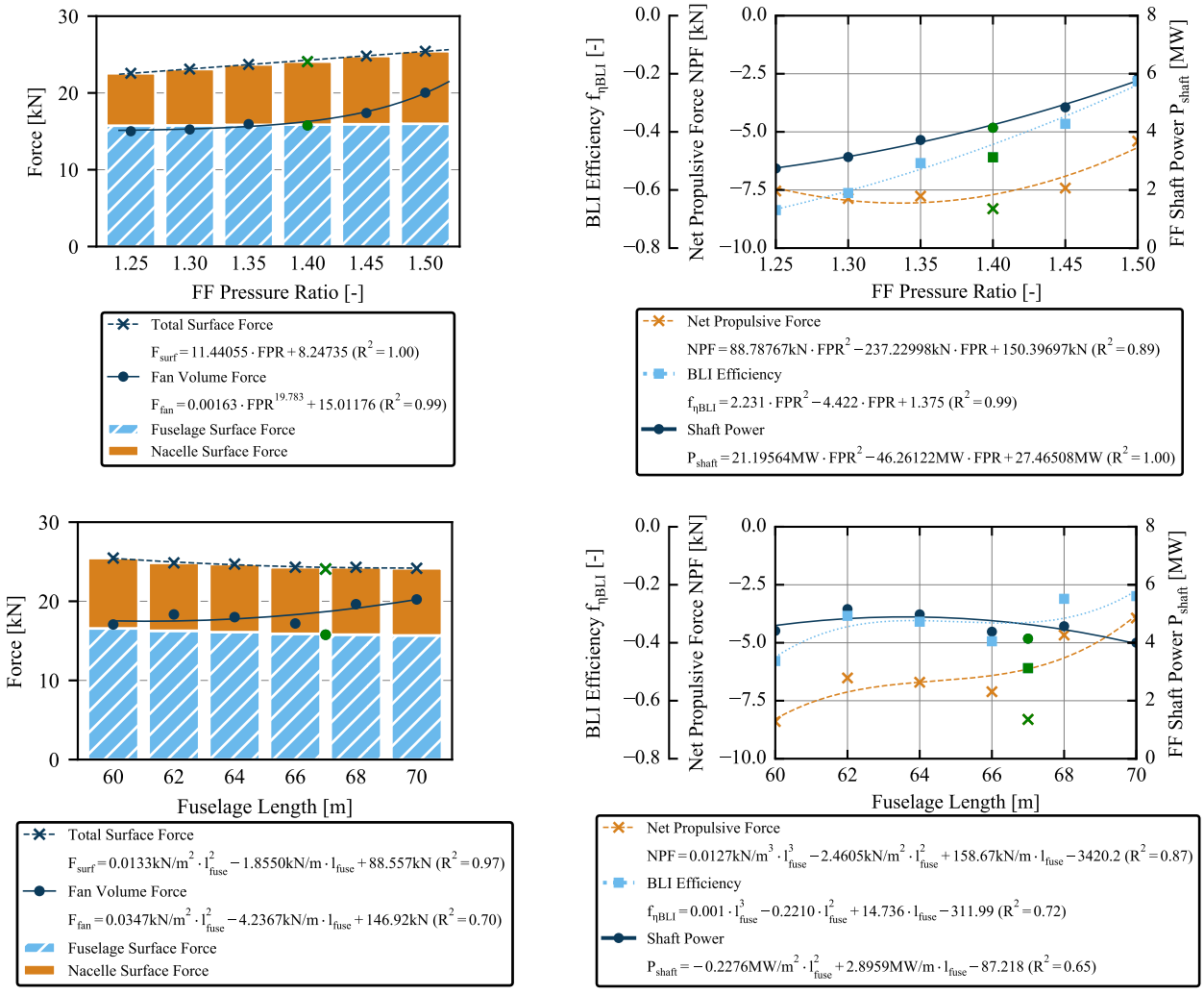

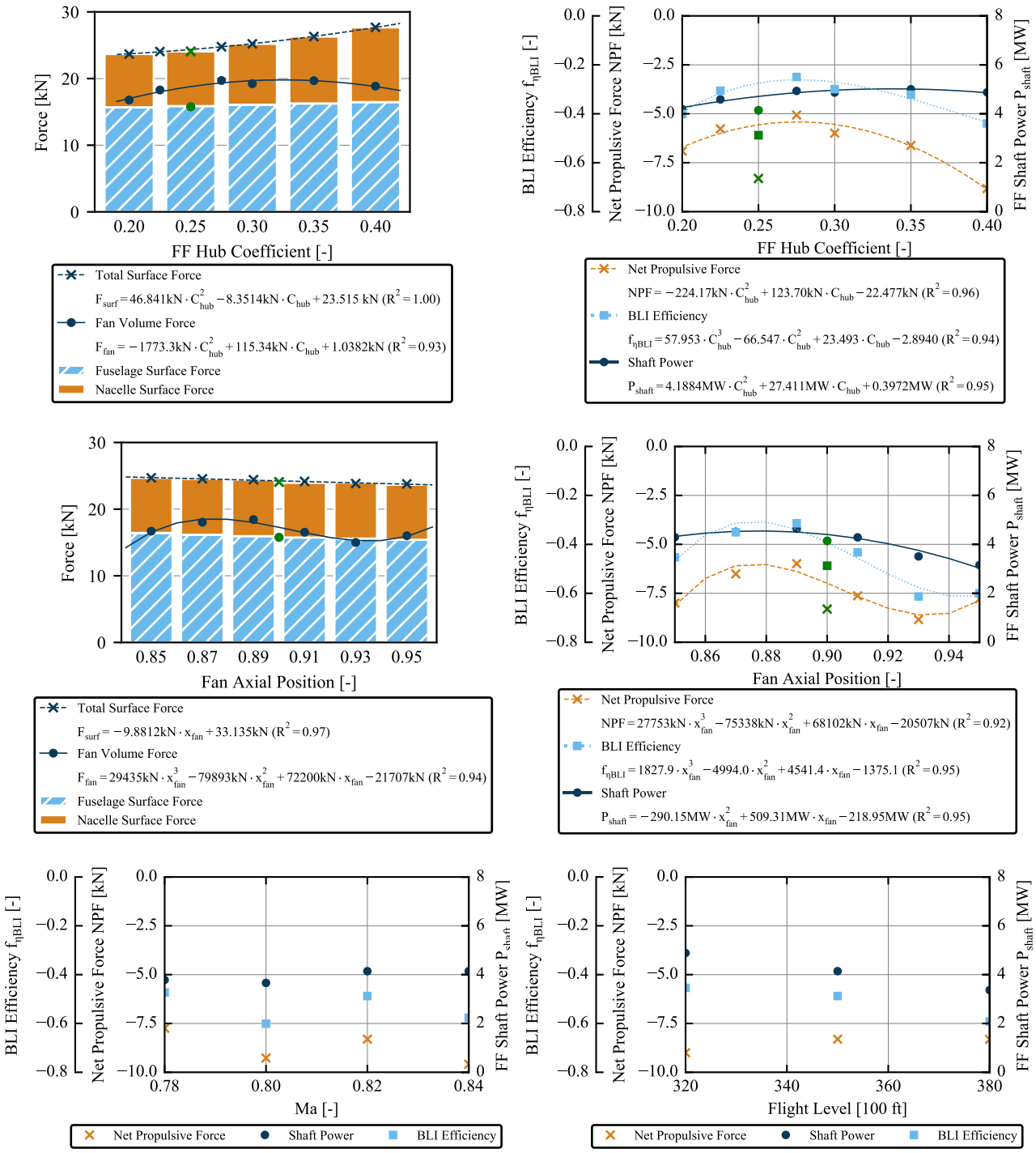

Fig. 10 Results of the sensitivity study – forces, shaft power and BLI efficiency factor.

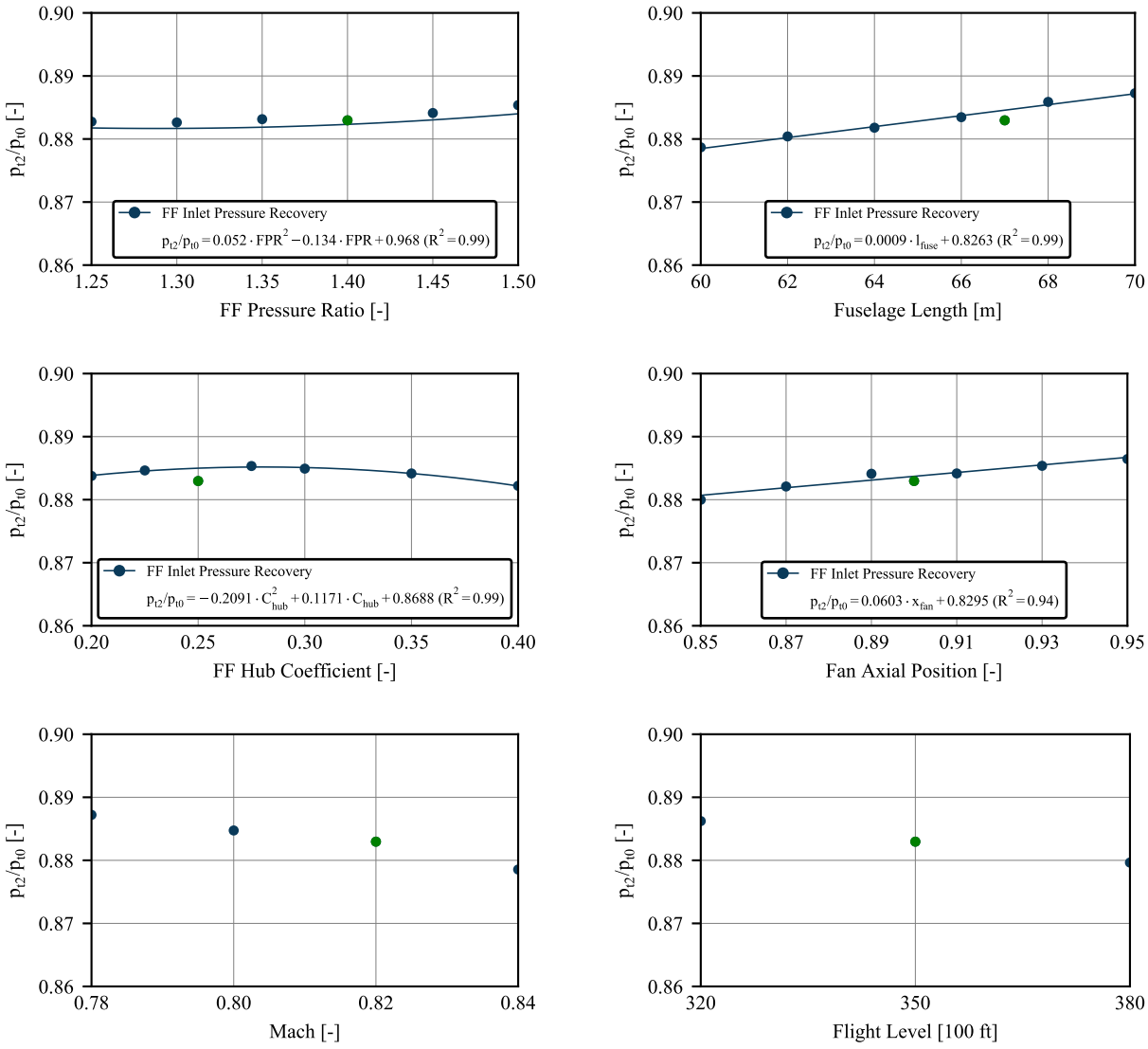

Fig. 11 Results of the sensitivity study – FF inlet total pressure recovery.